Journal of the Korean Physical Society, Vol. 55, No. 2, August 2009, pp. 661∼665

Modeling of the Cross-linking and the Diffusion Processes in a Negative Chemically Amplified Resist

Sang-Kon Kim,* Hye-Keun Oh, Young-Dae Jung and Ilsin An
Department of Applied Physics, Hanyang University, Ansan 426-791

(Received 3 January 2009)

A chemically amplified negative-type resist has proposed advantages of a negative tone imaging. However, a negative-image system has been analyzed virtually by using a positive-image simulation because the dark field of a positive-tone mask corresponds to the bright field of a negative-tone mask. In this paper, a new modeling method for the cross-linking and the diffusion processes is introduced for the lithography process of a negative resist. For random approaches, the gel formation model and the Monte Carlo method are described for negative resist. The simulated results for negative resists are in good agreement with the experimental results.

PACS numbers: 85.40.HP, 78.40.Fy, 78.20.Bh, 85.85.+j
Keywords: Microlithography, Lithography simulation, Negative chemically amplified resist, CAR, Monte Carlo method

I. INTRODUCTION

Numerous reports address simulation techniques, and many studies have focused, in particular, on chemically amplified positive-type resists (positive CAR) due to their role as mainstream resist materials used in the production of ICs. However, chemists and engineers have been able to provide a wide variety of resists, both negative and positive, to answer the needs of a growing industry. The choice of whether to use a negative or a positive resist system depends upon the needs of the specific application, such as resolution, ease of processing, and cost [1].

A negative resist, SU-8, has been widely used in the MEMS (micro electro mechanical system), IC packaging (bump, insulator, and encapsulation), soft lithography (micro mold, imprint), micro fluids (inkjet, micro reactor, and biochips), and optical device (waveguide, optical switch) fields [2]. For double patterning, the use of a bright field mask with a negative resist can provide a larger process window than the use of a dark field mask with a positive resist [3]. However, in most papers, the lithography process with a negative resist was modeled by fitting experimental results and was simulated by changing the dark field of a mask into the bright field of a mask in the modeling of the positive resist [4]. The development of modeling and simulation of the lithography process of a negative resist has helped to the development of new resists with high sensitivity, high resolution, and small LER (line edge roughness) and has allowed capitalization on the proposed advantages of negative tone imaging for printing narrow trenches.

In this paper, a new modeling method is introduced for the lithography process of a negative resist. Random approaches, such as the gel formation model and the Monte Carlo method, describe the post-exposure bake (PEB) process of the negative resist. The simulated results are compared with experimental results for accuracy.

II. MODELING OF THE LITHOGRAPHY PROCESS WITH A NEGATIVE RESIST

Chemically amplified negative-type resists generally contain components: a polymer and a photo / radio-sensitive compound called a photo-acid generator (PAG), and cross-linker. When a negative CAR is irradiated by using deep ultra-violet (DUV), the PAG generates an acid, and the acid catalyzes cross-linking reactions among the polymer chains directly or through the cross-linker during the PEB. The cross-linking leads to the formation of polymer clusters and finally to a gel state, which is considered insoluble in the developer. The developer dissolves single and uncross-linked polymer chains. As a result, the region of the resist film with the absorbed radiation becomes less soluble than the neighboring regions with the non-absorbed radiation. The neighboring regions dissolve faster and reveal the surface of the substrate. The cross-linking reaction caused by the photon energy generated in the exposure process is

$$\frac{d\,[S_{ci}]}{dt} = -k_{photo} \cdot [S_{ci}] \cdot I, \tag{1}$$

*E-mail: sangkona@hotmail.com; http://www.sangkon.info

where t is the exposure time, k_{photo} is the cross-linking reaction constant for the cross-linking reaction attributable to the photon energy generated by exposure, I is the intensity of the exposure light, and S_{ci} is the normalized concentration of the reactive groups in the cross-linking agent. For a negative CAR, exposing the resist to DUV light generates acid from the PAG:

$$\frac{d\left[PAG\right]}{dt} = -C \cdot \left[PAG\right] \cdot I, \tag{2}$$

$$\begin{aligned}\left[H^{+}\right]_{t} &= \left[PAG\right]_{t=0} - \left[PAG\right]_{t} \\ &= \left[PAG\right]_{t=0}\left(1 - e^{-CE}\right),\end{aligned} \tag{3}$$

where E is exposure dose and C is Dill's parameter. During PEB, the photo-generated acid catalyzes a thermally-induced reaction:

$$\frac{d\left[H^{+}\right]}{dt'} = -k_{loss} \cdot \left[H^{+}\right] + \nabla \cdot \left(D_{acid} \nabla \left[H^{+}\right]\right), \tag{4}$$

$$\frac{d\left[S_{ci}\right]}{dt'} = -k_{ci} \cdot \left[H^{+}\right]^{m} \cdot \left[S_{ci}\right], \tag{5}$$

where t' is the PEB time (sec), $[H^{+}]^{m}$ is the acid concentration, D_{acid} $(= k_{0\,acid} \exp\left(-E_{aacid}/RT\right))$ is the diffusion constant of the acid, m is the order of the cross-linking reaction, k_{ci} $(k_{0\,ci} \exp\left(-E_{aci}/RT\right))$ is the cross-linking reaction constant, k_{loss} $(= k_{0\,loss} \exp\left(-E_{aloss}/RT\right))$ is the constant corresponding to the deactivation of the acid in the PEB, and E_{aacid}, E_{aci}, and E_{aloss} indicate the activation energies.

III. RANDOM APPROACHES

1. Gel Formation Model

The cross-linking probability of any monomer, such as the relationship between the gel fraction and the cross-link density, can be described as a network formation. The cross-link density (q) is the probability for a monomer to be cross-linked. It determines the ratio of cross-linked monomers to the total number of monomers when the cross-links are formed randomly. The gel fraction (g) is the probability that a monomer is part of the gel. In the case of chain cross-linking inhibition, for a Poisson distribution of chain lengths,

$$q = \frac{k'd}{\delta_0}, \quad g = 1 - \frac{1}{\left[1 + qgf\left(g,i\right)/2\right]^{2}}, \quad \delta_0 \gg 0, \tag{6}$$

$$\begin{aligned}q = 1 - \exp\left(-\frac{k'd}{\delta_0}\right), \quad g = 1 - \frac{1}{\left[1 + qgf\left(g,i\right)/2\right]^{2}}, \\ otherwise,\end{aligned} \tag{7}$$

where δ_0 is the total number of available sites for cross-linking per chain, d is the exposure dose $\left(\mathrm{mJ/cm^2}\right)$, and the function $f\left(g,i\right)$ incorporates the chain reaction termination effect. The function $f\left(g,i\right)$ is $f\left(g,i\right) = \left(g + 2i/\left(1-i\right)\right)/\left(g + i/\left(1-i\right)\right)^{2}$, where $k' = k/i$, k is the inverse of the resist sensitivity $\left(\mathrm{cm^2/mJ}\right)$, and i is the inhibition activity. $f\left(g,i\right)$ is the probability that the length of a polymerizing chain terminates its increase, with $i\left(d\right) = a\left[\log\left(d\right)\right]^{2} + b$, where a and b are fitting constants [5].

2. Monte Carlo Method

The Monte Carlo method involves a representative random sampling of the abscissa instead of an evaluation of the photo- and thermal-chemical reaction at every one component of a CAR. During the exposure process, the probability P_{PAG} $\left(= \left[PAG\right]_{t=0}\left(1 - e^{-CE}\right)\right)$, that a PAG molecule is converted to acid is just equal to the relative fraction of PAG molecules that converted to acid. The probability P_{ci} $\left(= \left[S_{ci}\right]_{t=0}\left(1 - e^{-k_{photo}E}\right)\right)$, that the cross-linking reaction is caused by the photon energy generated in the exposure process is equal to the relative fraction of the reactive groups in the cross-linking agent. For PEB, since the master equation of the Monte Carlo process can be viewed as a gain-loss balance, the time derivatives of the average particle numbers without acid diffusion are

$$\begin{aligned}\frac{d\langle n_H\rangle}{dt} &= -k_2\langle n_H\rangle, \\ \frac{d\langle n_M\rangle}{dt} &= -k_1\left[\langle n_M\rangle\langle n_H\rangle + \alpha\left(n_M, n_H\right)\right],\end{aligned} \tag{8}$$

where k_1 is the acid-catalyzed protection rate, k_2 is acid loss reaction rate, $\alpha\left(n_M, n_H\right)$ is $\langle n_M, n_H\rangle - \langle n_M\rangle\langle n_H\rangle$, the average particle numbers are $\langle n_M\rangle = \sum_{n_M,\,n_H} n_M P\left(n_M, n_H\right)$ and $\langle n_H\rangle = \sum_{n_M,\,n_H} n_H P\left(n_M, n_H\right)$, P is the probability, n_H is the number of acid molecules, and n_M is the number of blocked polymer sites.

IV. ANALYSIS

When a negative-tone system is compared to a positive-tone system, one of the differences is the aerial image from mask. The dark field of a positive mask corresponds to the bright field of a negative mask. It is similar to comparing a contact hole pattern with an isolated line pattern in a positive-tone system. The other difference is the modeling of the resist process. The simulation model of a negative-tone process in the PEB includes a bulk acid loss, an acid diffusion, and a cross-linking reaction instead of the deprotection reaction in the model of a positive-tone process. Hence, a negative-tone process is different from a positive-tone process in optical and physical phenomena. When the pattern size is smaller

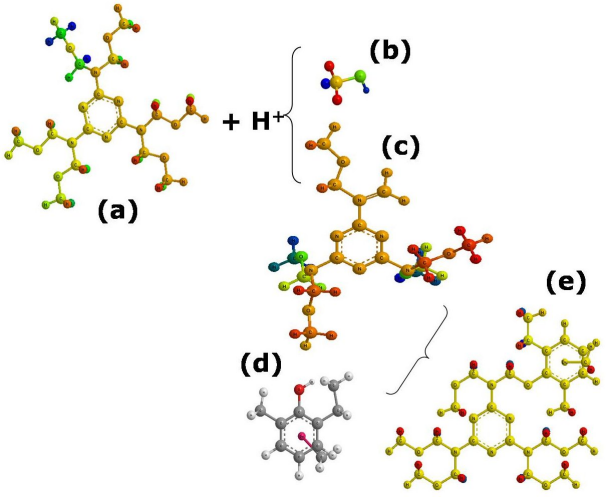

Fig. 1. Cross-linking mechanism for SAL 605 during PEB: (a) hexamethoxymethylmelamine, (b) HOCH3, (c) iminium ion, (d) novolac repeat unit, and (e) cross-linked polymer.

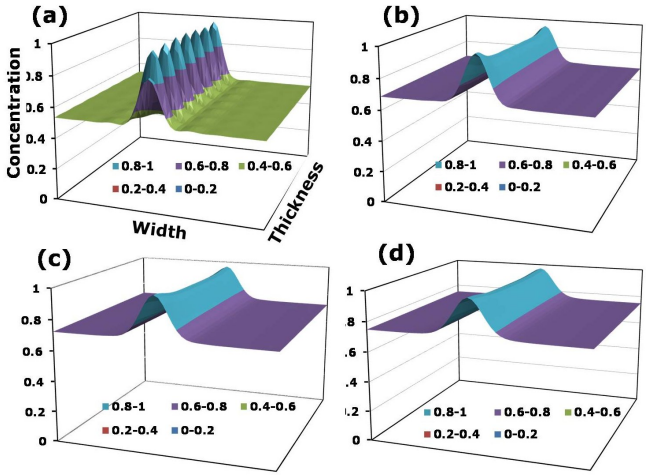

Fig. 2. Simulation results for the cross-linked polymer concentration of a negative CAR after PEB by using FTCS due to diffusion lengths of (a) 0.02-μm, (b) 0.025-μm, (c) 0.045-μm, and (d) 0.065-μm.

and an optical proximity correction (OPC) is required, the negative-tone process requires accurate modeling and simulation of a negative-tone resist.

Figure 1 shows the cross-linking mechanism for a commercial negative-tone CAR, SAL 605, during the PEB by using ChemOffice of CambridgeSoft Ins. A photogenerated acid must first encounter a lone pair on one of the oxygens of hexamethoxymethylmelamin (HMM), and cleavage occurs to produce methanol. These result in the creation of an iminium ion. A bimolecular reaction occurs between the iminium ion and a novolac [5].

Figure 2 shows the numerical simulation of a negative CAR in Eqs. (4) and (5) by using the forward time and

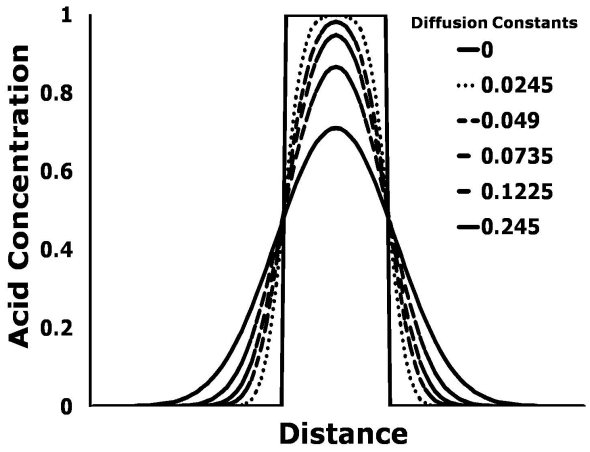

Fig. 3. Simulation results for acid diffusion for various diffusion constants by using FTCS.

centered space (FTCS). The numerical equations are

$$\frac{f_{i,j}^{n+1}-f_{i,j}^{n}}{\Delta t}=-k_{loss}f_{j}^{n} +D_{acid}\left(\frac{f_{i+1,j}^{n}-2f_{i,j}^{n}+f_{i-1,j}^{n}}{\Delta x^{2}} +\frac{f_{i,j+1}^{n}-2f_{i,j}^{n}+f_{i,j-1}^{n}}{\Delta y^{2}}\right), \tag{9}$$

$$f_{i,j}^{n+1}=f_{i,j}^{n}-cf_{j}^{n}+d_{1}\left(f_{i+1,j}^{n}-2f_{i,j}^{n}+f_{i-1,j}^{n}\right) +d_{2}\left(f_{i,j+1}^{n}-2f_{i,j}^{n}+f_{i,j-1}^{n}\right), \tag{10}$$

$$[S_{ci}]=[S_{ci}]_{t=0}\,e^{-k_{ci}f}, \tag{11}$$

where $f_{i,j}^{n}$ is $[H^{+}](t,x,y)$, c is $k_{loss}\Delta t$, t is $n\Delta t$, x is $i\cdot\Delta x$, y is $j\cdot\Delta y$, d_1 is $D_{acid}\Delta t/\Delta x^2$, and d_2 is $D_{acid}\Delta t/\Delta y^2$. The concentration of cross-linked polymer after the PEB is diffused more due to the increasing diffusion length. Simulation conditions are $k_{ci}=2.5$, $k_{amp}=0.75$, and $k_{loss}=2.3\times10^{-5}$.

Figure 3 shows the numerical simulation of acid diffusion for various diffusion constants by using FTCS. During the PEB, the relative acid concentration, H^+, due to Fick's second law is $d[H^+]/dt' = \nabla\cdot(D_{acid}\nabla[H^+])$ [6,7]. When the diffusion constant increases, acid is diffused more, so that the diffusion is one of the important effects of pattern formation.

Figures 4 and 5 show a comparison of the simulation results for positive and negative CAR processes for 82-nm line and space (L / S) pattern formation. The simulation results of a positive CAR in Fig. 4 are the aerial image, PAG concentration after exposure process, inhibitor concentration after PEB, and dissolution rate concentration for development [8,9].

Simulation results for a negative CAR in Fig. 5 are the aerial image, PAG concentration after exposure process, cross-linked polymer concentration after PEB, and dissolution rate concentration for development. For the same pattern formation, the aerial image of the negative

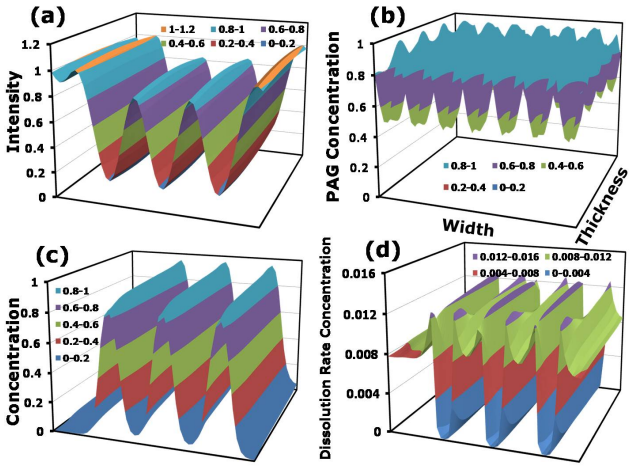

Fig. 4. Simulation results of positive CAR processes for 82-nm line and space pattern formation: (a) aerial image, (b) PAG concentration, (c) inhibitor concentration, and (d) dissolution rate concentration.

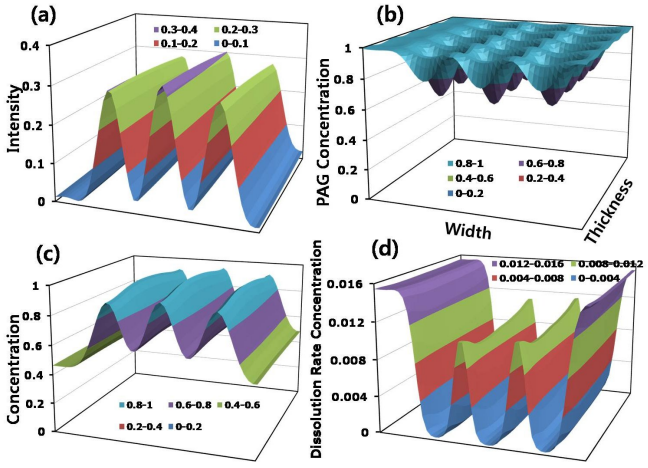

Fig. 5. Simulation results of negative CAR processes for 82-nm line and space pattern formation: (a) aerial image, (b) PAG concentration, (c) cross-linked polymer concentration, and (d) dissolution rate concentration.

process in Fig. 5(a) is opposite to that of the positive process in Fig. 4(a), but for a cross-linked polymer and dissolution rate concentration, the graphs of the negative process in Figs. 5(c) and (d) are similar to those of the positive process in Figs. 4(c) and (d).

Figure 6 shows a comparison of simulated and experimental results. For a comparison of 83-nm L / S pattern formation in Figs. 6(a) and (b), simulation conditions are a resist of 90-nm ARC thickness and 210-nm resist thickness, a 6% attenuated phase-shifting mask, a 0.75 NA, an annular illumination with an outer 0.89 σ and an inner 0.55 σ, a 25.6 mJ/cm^2 exposure, a post-apply bake (PAB) at 105 °C for 60 sec, a PEB at 105 °C for 60 sec, and development for 60 sec [10]. The simulation results in Fig. 6(b) are good agreement with the experimental

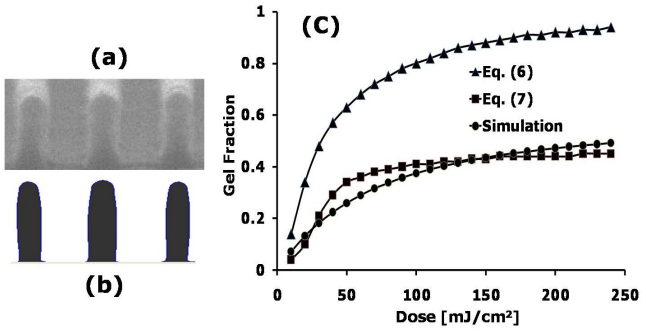

Fig. 6. Comparison of (b) resist-profile simulation to (a) the experimental SEM image with 83-nm L / S patterns [10], (c) Comparison of simulated and experimental gel fractions [5].

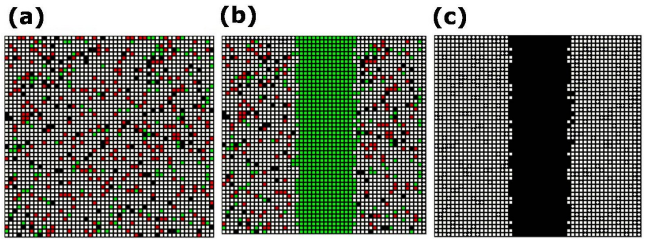

Fig. 7. Monte Carlo simulation of the placement, generation, and diffusion of photoacids in a molecular resist: (a) initial mixed distribution with acid distribution (5.04%), PAG distribution (10.48%), and inhibitor distribution (5.4%), (b) mixed distribution after exposure, and (c) cross-linked polymer distribution after 30 sec of PEB in a 2-dimensional plane (100-nm × 100-nm).

results in Fig. 6(a). For a comparison of the experimental gel fraction [5], the simulation results are compared with the results of the experimentally fitted gel function due to a modified exposure dose. The simulated gel fraction matches well with that of Eq. (7) rather than that of Eq. (6). Hence, the simulation results are reliable because the experimentally fitted function leads to the simulated gel fraction.

Figure 7 shows Monte Carlo simulation results of the lithography process in the two-dimensional plane (100-nm × 100-nm) of a negative molecular resist. A 32-nm line pattern is formed in a resist with a mixed distribution of acid (5.04%), PAG (10.48%), and cross-linked polymer (5.4%) by using the cross-linked mechanism of the random process. Hence, random approaches, such as the gel formation model and the Monte Carlo method, can describe the phenomenon and mechanism of a negative resist in the lithography process.

V. CONCLUSION

The mechanism of a negative-tone system is not a change of the dark field of a positive mask into to the

bright field of a negative mask. The negative-tone process is different from the positive-tone process in optical and physical phenomena. For a negative resist, a new modeling method with cross-linking and diffusing processes and the random approaches, such as the gel formation model and the Monte Carlo method, are described. For 83-nm pattern formation, the internal results, such as photo-acid generation and cross-linked polymer concentrations, of the positive and the negative processes are compared with each other. For confidence with negative-tone modeling and simulation, an 83-nm line and space pattern profile and the simulated gel fraction are compared with those of experiment. Simulated results match the experimental results well.

ACKNOWLEDGMENTS

This research was supported by Basic Science Research Program through the National Research Foundation on Korea (NRF) funded by the Ministry of Education, Science and Technology (2009-0074676).

REFERENCES

[1] J. M. Shaw, J. D. Gelorme, N. C. LaBianca, W. E. Conley and S. J. Holmes, IBM J. Res. Develop. **41**, 81 (1997).
[2] Y. Washio, T. Senzaki, Y. Masuda, K. Saito and H. Obiya, Proc. SPIE **5753**, 959 (2005).
[3] R.-H. Kim, T. Wallow, J. Kye, H. J. Levinson and D. White, Proc. SPIE **6520**, 65202M (2007).
[4] Y. Sensu, A. Sekiguchi and Y. Kono, Proc. SPIE **6153**, 61533S (2006).
[5] G. P. Patsis and N. Glezos, J. Vac. Sci. Technol. B **20**, 1303 (2002).
[6] S.-K. Kim and H.-K. Oh, J. Korean Phys. Soc. **53**, 2682 (2008).
[7] S.-K. Kim, H.-K. Oh, Y.-D. Jung and I. An, J. Korean Phys. Soc. **54**, 1685 (2009).
[8] S.-K. Kim, J. Korean Phys. Soc. **49**, 1211 (2006).
[9] S.-K. Kim and H.-K. Oh, J. Korean Phys. Soc. **51**, 1413 (2007).
[10] K. Patel, M. Lawson, P. Varanasia, D. Medeirosb, G. Wallraff, P. Brock, R. DiPietroc, Y. Nishimura, T. Chibad and M. Slezake, Proc. SPIE **5376**, 536874 (2004).